Chapter 7

Archaeal tetraether membrane lipid fluxes in the northeastern Pacific and the Arabian Sea: Implications for TEX_{86} paleothermometry

Cornelia Wuchter, Stefan Schouten, Stuart G. Wakeham* and Jaap S. Sinninghe Damsté

Submitted to *Paleoceanography*

Abstract.

The newly introduced temperature proxy TEX_{86} is based on the number of cyclopentane moieties in the glycerol dialkyl glycerol tetraethers (GDGTs) lipids of marine Crenarchaeota which change as a function to temperature. The GDGT signal used for TEX_{86} paleothermometry found in sediments reflect sea surface temperature (SST). However, marine Crenarchaeota occur ubiquitously in the world oceans over a large depth range and until now only work done on suspended particulate organic matter (POM) confirmed that the TEX_{86} in depth correlates well with SST. We analysed the GDGT distribution in settling POM using sediment traps from the northeastern Pacific Ocean and the Arabian Sea to investigate the seasonal and spatial distribution of the fluxes of crenarchaeotal GDGTs and the TEX_{86} signal which is transported to the sediment. At both settings the obtained TEX_{86} at all trap deployment depth reflects SST. At the Arabian Sea time series the TEX_{86} in the shallow trap at 500 m followed the in situ SST with an offset of about 3 weeks due to the settling speed of the GDGTs. This revealed that the GDGT signal which reaches deeper water is derived from the upper water column and reflect SST. The GDGT temperature signal in the deep traps at 1500 m and 3000 m do not show seasonal cycle but reflected annual mean SST. This is probably due to lateral transport of particles and associated mixing.

7.1 Introduction

Recently a new organic geochemical sea surface temperature proxy, the TetraEtherIndex of lipids with 86 carbon atoms (TEX_{86}) was proposed [*Schouten et al.,* 2002]. This new proxy is based on the number of cyclopentane moieties in the tetraether membrane lipids of marine Crenarchaeota. Marine Crenarchaeota are prokaryotes belonging to the domain of the Archaea. They are ubiquitously distributed in the world's ocean [*Fuhrman et al.,* 1992; *DeLong,* 1992; *Hoefs et al.,* 1997; *Sinninghe Damsté et al.,* 2002a] and it was estimated that marine Crenarchaeota comprises ca. 20% of all picoplankton in marine environments [*Karner et al.,* 2001].

Crenarchaeota possess unique membrane lipids which consist of glycerol dibiphytanyl glycerol tetraethers (GDGTs) [*DeRosa and Gambacorta* 1988] (see Fig.1 for structures). *Schouten et al.* [2002] showed that the distribution of marine crenarchaeotal GDGTs in core top sediments derived from different geographic locations correlate well with SST (Table 1). In cold areas the GDGT distribution is dominated by GDGT I and crenarchaeol (V). In warmer regions the GDGT distributions differ substantially as crenarchaeol is the most abundant GDGT and higher amounts of 1-3 cyclopentane-containing GDGTs (II-IV) and a regio-isomer of crenarchaeol (VI) are detected.

The increase of cyclopentane moieties in the membrane lipids of thermophilic Crenarchaeota, close phylogenetic relatives of the marine Crenarchaeota, is considered to be a temperature adaptation mechanism of the cell membrane [*Gliozzi et al.,* 1983, *Uda et al.,* 2001]. Recent mesocosm studies confirmed that marine Crenarchaeota inherited a similar way of temperature adaptation from their hyperthermophilic ancestors [*Wuchter et al.,* 2004]. With increasing temperature an increase in the number of cyclopentane moieties was observed in the GDGT membrane lipids of marine Crenarchaeota. 16S rDNA analyses revealed that a single crenarchaeotal species, derived from North Sea waters, was present in the incubated mesocosm tanks and that the changing GDGT distribution reflected a physiological adaptation. The obtained TEX_{86} equation from the mesocosm studies had a similar slope but differed in the intersection to the y axes compared to the core top equation (Table 1). This offset in the slope of the equation was caused by a relatively low amount of the regio-isomer of crenarchaeol. This GDGT was less pronounced in the cold water crenarchaeotal species,

cultivated in the laboratory, compared to crenarchaeotal species which dwell in warmer environments.

The observed correlation of TEX_{86} in core top sediments with annual mean SST suggests that the marine crenarchaeotal lipid signal is predominantly biosynthesized in the upper part of the water column. This is supported by our study of GDGT distributions in suspended particulate organic matter (POM) from different oceanic regions [*Wuchter et al.*, 2005], which revealed that the TEX_{86} correlates well with the upper 100m water column temperature (Table 1). GDGTs from the photic zone are probably much more effectively transported to the sediment by grazing and repackaging in large particles than GDGTs from deeper waters. The obtained equation for suspended POM samples was similar to the core top equation although there was a larger amount of scatter apparent compared to the core top equation. This was probably caused by contributions of both living and dead cell material of marine Crenarchaeota [*Wuchter et al.*, 2005]. The POM samples represented a mixture of fine suspended material, with negligible settling velocities and long residence time in the water column, and rapid sinking particles with a high settling rate [*Wakeham and Canuel* 1988].

Our previous studies established that the TEX_{86} in suspended POM is strongly correlated with SST. However, it has not been demonstrated yet how and when the signal produced in the water column is transported to the sediment floor. For this the fluxes of GDGTs through the water column need to be determined using sediment traps. Sediment traps are used to sample the flux of particulate organic matter which is derived from the surface waters mostly at time of high productivity [*Wakeham and Lee* 1993]. In this study, we analyzed the GDGT distribution in settling particulate organic matter using sediment traps from the northeastern Pacific Ocean and the Arabian Sea to investigate the seasonal and spatial distribution of the fluxes of crenarchaeotal GDGT and TEX_{86} signal transported to the sediment.

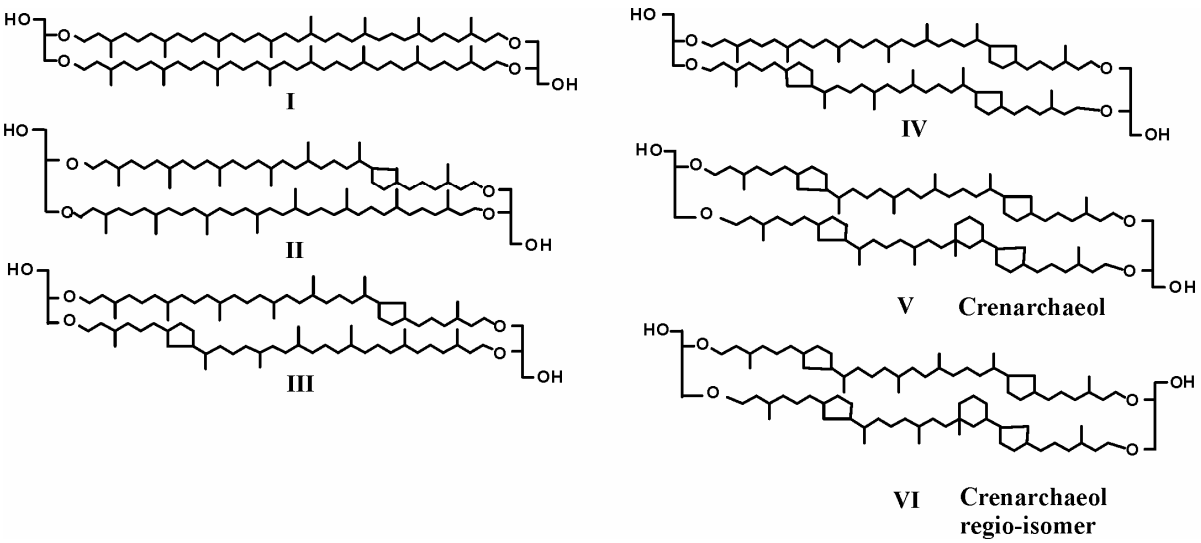

Figure 1. Structures of GDGT membrane lipids of marine pelagic Crenarchaeota.

origin	equation	r^2	sample amount
core tops	TEX_{86}= 0.015*T+0.29	0.92	n= 61
mesocosm experiment	TEX_{86}= 0.015*T+0.10	0.79	n= 16
POM from upper 100m	TEX_{86}= 0.017*T+0.29	0.80	n= 65

Table 1. Comparison of the TEX_{86} equations obtained from core top sediments [*Schouten et al.,* 2002], the mesocosm experiment [*Wuchter et al.,* 2004] and POM from different oceanic provinces [*Wuchter et al.,* 2005].

7.2 Material and Methods

7.2.1 Study sites and collection of samples

7.2.2 Northeastern Pacific

During June 1984 sediment traps were deployed in the northeastern Pacific at two stations. One station was located in the oligotrophic center of the northeastern Pacific Ocean at 33.3°N, 139.2°W [VERTEX 5A, *Silver and Gowing* 1991] and the other station was located in the upwelling area near the Californian coast at 36.1°N, 122.6°W [VERTEX 5C, *Silver and Gowing* 1991]. Free floating Soutar-type particle interceptor traps [for details see *Wakeham and Canuel* 1988], with a collecting area of 0.25 m^2, were used to collect rapidly sinking, large particles over four different depth intervals (100 m, 250 m, 750 m and 1500 m). The sinking particles were size fractioned in >300 µm and <300 µm. Trap deployment periods were 22 days for the oligotrophic setting and 13 days for the upwelling station. Mercury chloride was used to inhibit decomposition of the material in the traps.

7.2.3 Arabian Sea

The sampling site in the Arabian Sea was located approximately 350 km offshore of the Omani coast (MS-3: 17º12'N, 59º36'E) at a water depth of 3465 m. Three trap arrays at depth of ~500 m, ~1500 m and ~3000 m with varying module configurations (wide mouth traps with 0.37 m^2 collecting areas and narrow mouth traps with 0.018 m^2 collecting areas) were deployed in November 1994 (R/V *Thomas G. Thomson* cruise TN041), serviced and redeployed in May 1995 (cruise TN047) and recovered after a second time segment in January 1996 (cruise TN050). Carousels in the traps were programmed to collect sinking material over variable time intervals, ranging from 8.5 to 34 days. Shorter intervals were set for monsoon periods when higher fluxes were expected. In total for each depth 22 time-resolved samples were recovered. To inhibit decomposition mercuric chloride was used as a biocide (Lee et al 1992). For more detailed information about the Arabian Sea setting see *Wakeham et al.* [2002].

7.2.4 GDGT analysis

The sediment-trap samples were split and the lipid fraction was filtered over muffled glass fiber filters and Soxhlet extracted with dichloromethane (DCM) and methanol (2:1 by

volume) at Skidaway Institute of Oceanography (for details see *Wakeham et al*., 2002). An aliquot of the total lipid extract was cleaned over an activated Al_2O_3 column by eluting with methanol/DCM (1:1 by volume). For analysis of GDGTs, the solvent was removed under a stream of nitrogen and the residue was dissolved by sonication (5 min) in hexane/propanol (99:1 by volume). The resulting suspension was filtered through a 0.45-µm-pore-size, 4 mm diameter Teflon filter prior to injection. The intact GDGTs were analyzed by high performance liquid chromatography (HPLC) - atmospheric pressure positive ion chemical ionization mass spectrometry (APCI-MS) by applying conditions slightly modified from *Hopmans et al.* [2000]. Analyses were performed using an HP (Palo Alto, CA, USA) 1100 series LC-MS equipped with an auto-injector and Chemstation chromatography manager software. Separation was achieved on a Prevail Cyano column (2.1 x 150 mm, 3 µm; Alltech, Deerfield, IL, USA), maintained at 30°C. Injection volumes were 15 µl. GDGTs were eluted isocratically with 99% A and 1% B for 5 min, followed by a linear gradient to 1.8% B in 45 min, where A = hexane and B = propanol. Flow rate was 0.2 ml/min. After each analysis the column was cleaned by back-flushing hexane/propanol (90:10, by volume) at 0.2 ml/min for 10 min. Detection was achieved using APCI-MS of the eluent. Conditions for APCI-MS were as follows: nebulizer pressure 60 psi, vaporizer temperature 400 °C, drying gas (N_2) flow 6 l/min and temperature 200 °C, capillary voltage -3 kV, corona 5 µA (~ 3.2 kV). GDGTs were detected by single ion monitoring of their $[M+H]^+$ ions (dwell time 237 ms) and quantified by integration of the peak areas and comparison with a standard curve of a Crenarchaeol standard.

For TEX_{86} calculation the peak areas of GDGTs I-VI were integrated and TEX_{86} values were calculated according to the index from *Schouten et al.,* [2002] which was defined as follows:

$TEX_{86} = (III+IV+VI) / (II+III+IV+VI)$. [1]

For the temperature correlation only TEX_{86} values were used where all isomers of GDGTs could be detected in sufficient abundances. TEX_{86} temperatures were calculated using the correlation obtained by *Schouten et al.* [2002]:

$TEX_{86} = 0.015*T+0.28$, ($r^2 = 0.92$) with T = annual mean SST (in °C). [2]

7.3 Results

The crenarchaeotal GDGT flux and distribution at different depths was analysed at two different settings in the northeastern Pacific during June 1984 and during the annual cycle at one station in the Arabian Sea in 1995. These data were used to investigate the variation with depth of the fluxes of crenarchaeotal GDGT and the TEX_{86} signal which is transported to the sediment. The station in the Arabian Sea also provided information on the seasonal flux of GDGTs and seasonality of the TEX_{86} signal.

7.3.1 GDGT flux and TEX_{86} signal in the northeastern Pacific

At the oligotrophic station in the northeastern Pacific GDGT fluxes between 0.2 and 4 µg GDGTs m^{-2} day^{-1} were measured. The maximum GDGT fluxes was measured at 750 m depth with about 4 µg GDGTs m^{-2} day^{-1} in the size fraction <300 µm (Fig. 3). Generally, higher GDGT fluxes were measured below 100 m depth and in the trap fraction <300µm (Fig. 2a). At 1500 m the GDGT flux was substantially lower with less than 0.5 µg GDGTs m^{-2} day^{-1} (Fig. 2a). At the 100m trap 22 % of the GDGT flux was derived from the >300µm fraction (Fig. 2a). With increasing depth the percentage of >300 µm fraction in the flux increased to 41 % at 250 m and 32 % at the 750 m trap. The TEX_{86} varied between 0.56 and 0.64 with highest TEX_{86} values in the 250 m traps (Table 2). TEX_{86} values between the different size fractions showed no substantial difference at the same depth (Table 2). The average TEX_{86} was 0.59 ± 0.04 at this station.

For the upwelling station GDGT fluxes varied between 5 µg and 4.3 mg GDGTs m^{-2} day^{-1}. The maximum GDGT flux was measured at 1500 m depth with about 4.3 mg GDGTs m^{-2} day^{-1} (Fig. 2b). The GDGT flux at the 100 m depth trap was ca. 60 µg GDGTs m^{-2} day^{-1} for the fraction <300 µm and comprised 93 % of the GDGT flux. The fraction >300 µm represented only 7% of the GDGT flux. The trap deployed at 250 m showed similar fluxes of ca. 40 µg GDGTs m^{-2} day^{-1} for both size fractions (Fig. 2b). At 750 m a higher flux was measured for the fraction <300 µm with about 100 µg GDGTs m^{-2} day^{-1} comprising 67 % of the GDGT flux (Fig. 2b). The fraction >300 µm at the same depth had a flux of about 60 µg GDGTs m^{-2} day^{-1} (Fig. 2b). The TEX_{86} varied between 0.45 and 0.54 and the average TEX_{86} was 0.50 ±0.03. Generally there was no substantial difference in the TEX_{86} from both size fractions of descending particles derived from the same depth (Table 2).

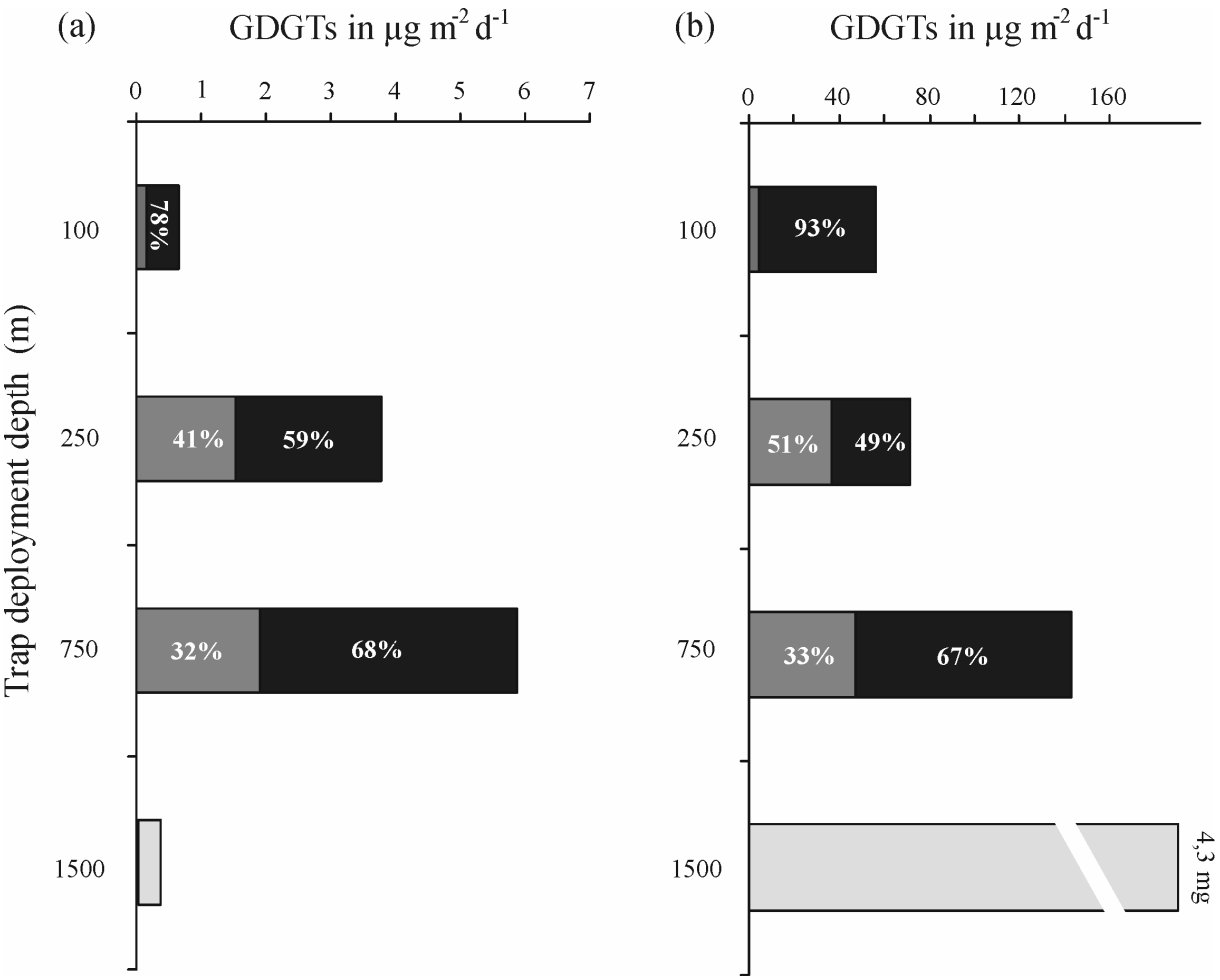

Figure 2. GDGT fluxes in different depth and size classes in the northeastern Pacific Ocean. Traps were deployed (a) in an oligotrophic setting and (b) at an upwelling site near the Californian Coast. Grey shaded bars represent the size fraction > 300 µm and black bars represent size fraction < 300 µm. White number in bars represent the percentage of the different size fractions of the total GDGT flux. White bars represent combined fractions at 1500 m deployment depth.

	depth (m)	TEX_{86} > 300um	TEX_{86} < 300um	TEX_{86} temperature (°C) > 300um	TEX_{86} temperature (°C) < 300um	mean *in situ* temp.(°C)	annual mean SST (°C)
oligotroph	100m	n.d	n.d	n.d	n.d	18	
	250m	0.64	0.60	23.3	20.7	10	
	750m	0.57	0.56	18.7	18.0	4.5	
	1500m		n.d		n.d	2.8	**20**
	average	**0.61**	**0.58**	**21.0**	**19.4**		
	Std.	**0.05**	**0.03**	**3.3**	**1.9**		
upwelling	100m	0.51	0.52	14.7	15.3	9	
	250m	0.54	0.49	16.7	13.3	7	
	750m	0.45	0.46	10.7	11.3	4.5	**14**
	1500m		0.52[a]		15.3[a]	2.8	
	average	**0.50**	**0.50**	**14.0**	**13.8**		
	Std.	**0.05**	**0.03**	**3.1**	**1.9**		

Not determined (n.d.) were samples with too low amount of GDGTs for reliable TEX_{86} calculation

(a) at the 1500 m trap both size fractions were combined

Table 2. TEX_{86} values and calculated TEX_{86} temperature compared to annual mean SST at the two sampling sites at the northeastern Pacific Ocean.

7.3.2 GDGT fluxes and TEX_{86} in the Arabian Sea

GDGT fluxes in the Arabian Sea showed a strong seasonality. At all three trap deployment depths (500, 1500, and 3000 m) the highest fluxes of GDGTs were measured during the monsoon periods with the highest fluxes during the south-west monsoon (SWM) (Fig. 3a). In the 500 m trap the maximum GDGT flux was about 20 µg GDGTs m^{-2} day^{-1} during the SWM and about 14 µg GDGTs m^{-2} day^{-1} during the north east monsoon (NEM) (Fig. 3a). During the summer inter-monsoon (SI) and fall inter-monsoon (FI) the fluxes were generally low with fluxes of 0.2 - 5 µg GDGTs m^{-2} day^{-1} during the SI (Fig.3a). In the trap deployed at 1500 m the GDGT fluxes were generally twice as high as in the 500 m trap. Maximum GDGT fluxes of ~40 µg GDGTs m^{-2} day^{-1} were found during the SWM and ca. 20 µg GDGTs m^{-2} day^{-1} during the NEM in this trap (Fig. 3a). During the SI and FI the fluxes were lower varying between 2-13 µg GDGTs m^{-2} day^{-1}. Compared to the other two traps, the GDGT flux was lowest in the trap deployed at 3000 m and varied between 2-9 µg GDGTs m^{-2}

day^{-1} with maximum fluxes in the SWM (Fig. 3a). The seasonal change in the flux of GDGTs was less pronounced in the 3000 m trap compared to the shallower traps.

The TEX_{86} varied between 0.67- 0.75 at the 500 m trap, at the 1500 m trap between 0.66-0.74 and between 0.66-0.71 at the 3000 m trap (Table 3). In the trap deployed at 500 m a pronounced seasonal variation in the TEX_{86} signal is observed (Fig. 4a). This seasonal variation in the TEX_{86} was less pronounced in the 1500 m depth trap (Fig. 4b) and the 3000 m trap (Fig. 4c).

7.4 Discussion

7.4.1 Variation in GDGT fluxes with depth in the water column

At both investigated sampling sites GDGT fluxes increased below 100 m depth and maximum GDGT fluxes were measured in the Arabian Sea in the mid- water trap at 1500 m in the Arabian Sea (Fig. 3) and in the Northeastern Pacific at 750 m trap at the oligotrophic site and at 1500 m trap in the upwelling area (Fig. 2).

Deep water flux maxima for particles and lipids were reported previously in other oceanic settings [see *Wakeham and Lee* 1993 for references] and several processes have been invoked to explain this distribution. The accumulation of sinking particles at density discontinuities within the water column could create this distinct distribution [*Karl et al.,* 1976]. Also the input of fecal matter from migrating zooplankton populations into deeper water layers [*Urrère and Knauer* 1981, *Karl and Knauer* 1984] could cause deep water flux maxima. In the northeast Pacific at both investigated sampling sites a similar increase in the ratio of GDGTs derived from the larger size fraction was observed in water below 100 m depth (Fig. 2).The GDGTs in the larger size fraction are probably derived from fecal pellets of vertically migrating zooplankter in deeper waters. This supports previous studies where high fecal pellet fluxes were reported in mesopelagic waters at both sampling sites of the northeastern Pacific [*Silver and Gowing* 1991].

In the Arabian Sea vertical migration of zooplankton even in the oxygen minimum zone was reported previously [*Smith et al.,* 1998, *Wishner et al.,* 1998]. This migration behavior could be responsible for fecal pellet transport into the mid- water trap, bypassing the trap at 500 m depth. Horizontal advective processes such as lateral transport probably also play an important role in the distribution of organic matter into deep waters [*Karl and Knauer*

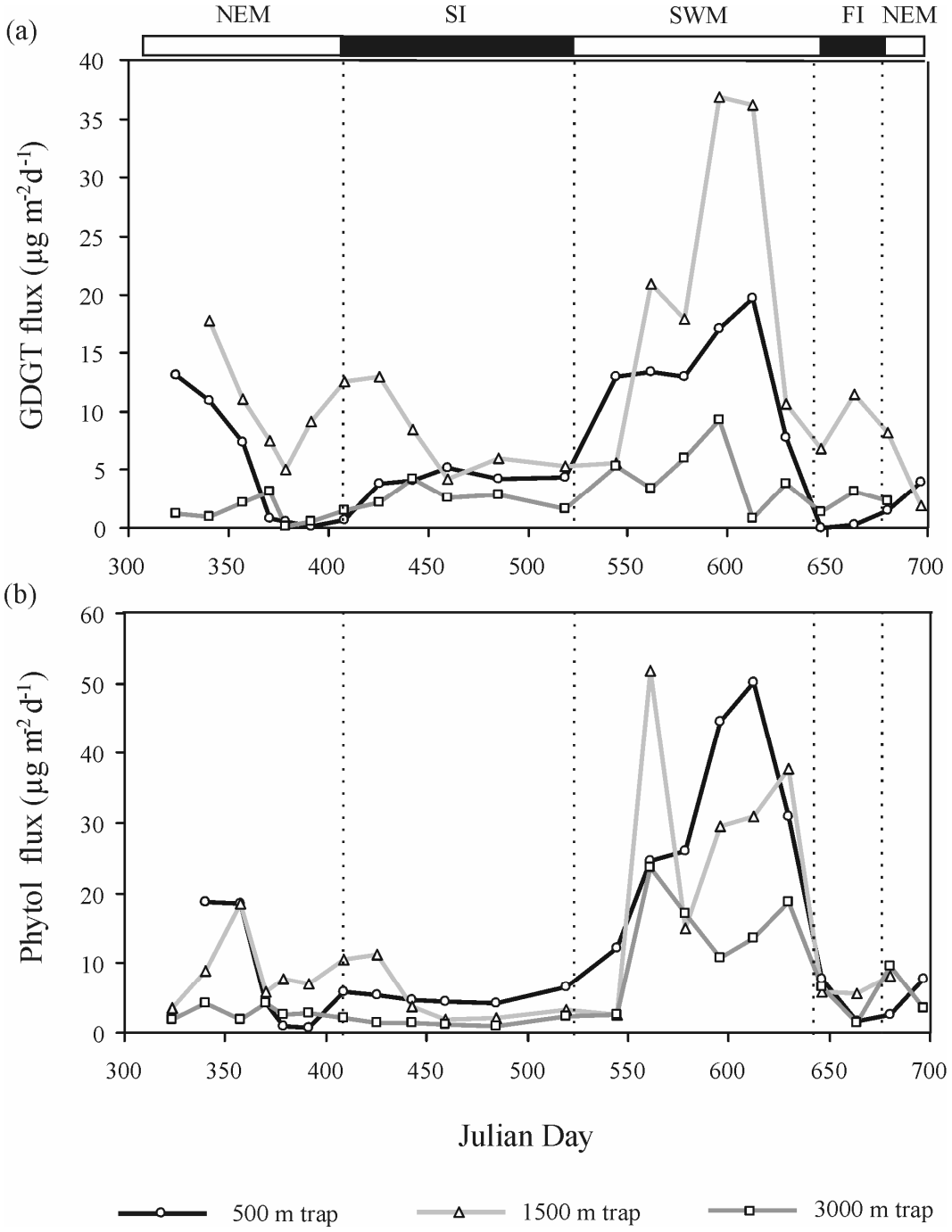

Figure 3. (a) GDGT and (b) phytol fluxes for the IRS-C traps at MS-3 in the Arabian Sea. Source data for phytol fluxes are obtained from http://usjgofs.whoi.edu/jg/dir/jgofs/arabian/. Bars at the top of the plot and dotted vertical lines indicate the monsoon periods based on *Weller et al.,*[1998]. NEM: North East monsoon, SI: Spring Inter-monsoon, SWM: South West monsoon, FI: Fall Inter-monsoon. Data points represent the center of collection intervals. The black line represent the shallow trap at ~500 m, the light grey correspond to the mid-trap at ~1500 m and the dark grey line represent the deep trap at ~3000 m depth.

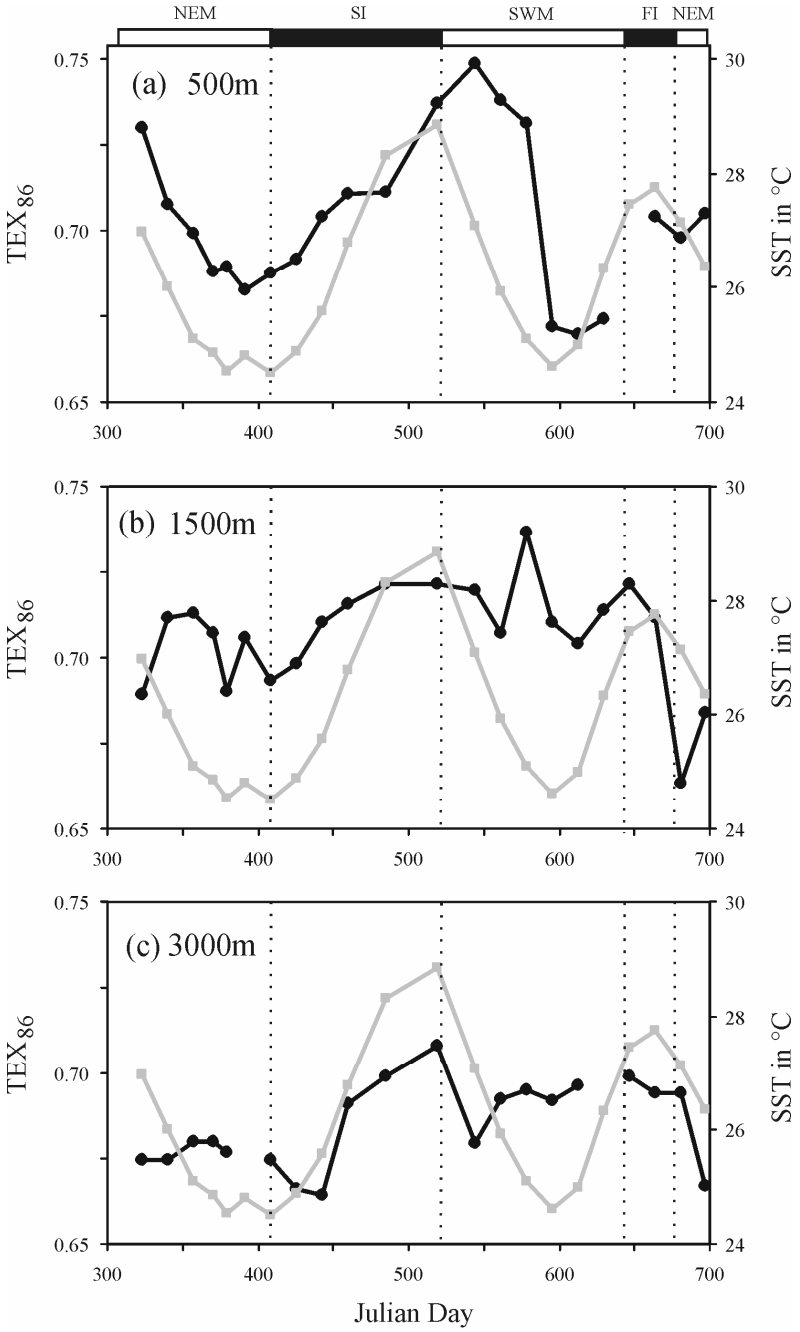

Figure 4. Seasonal variations in TEX_{86} and calculated SSTs in traps deployed at (a) 500 m, (b) 1500 m, (c) 3000 m depth at MS-3 station in the Arabian Sea. The black lines represents TEX_{86} values obtained at the different depths. Missing data points represent samples with insufficient amounts of GDGTs for TEX_{86} calculation. The grey lines represent integrated SST per deployment period. SST data were obtained from the pathfinder Advanced Very High Resolution Radiometer (AVHRR) data set at http: podaac.jpl.nasa.gov.

Julian Day	Average SST (°C)	500 m trap		1500 m trap		3000 m trap	
		TEX_{86}	TEX_{86} T (°C)	TEX_{86}	TEX_{86} T (°C)	TEX_{86}	TEX_{86} T (°C)
315 -332	27.0	0.73	29.3	0.69	26.6	0.67	25.6
332 -349	26.0	0.71	27.8	0.71	28.1	0.67	25.6
349 -366	25.1	0.70	27.3	0.71	28.2	0.68	26.0
366 -375	24.9	0.69	26.5	0.71	27.8	0.68	26.0
375 -383	24.5	0.69	26.6	0.69	26.7	0.68	25.8
383 -400	24.8	0.68	26.2	0.71	27.7	n.d.	n.d.
400 -417	24.5	0.69	26.5	0.69	26.9	0.67	25.6
417 -434	24.9	0.69	26.8	0.70	27.2	0.67	25.1
434 -451	25.6	0.70	27.6	0.71	28.0	0.66	24.9
451 -468	26.8	0.71	28.0	0.72	28.4	0.69	26.7
468 -502	28.3	0.71	28.1	0.72	28.8	0.70	27.3
502 -536	28.8	0.74	29.8	0.72	28.8	0.71	27.9
536 -553	27.1	0.75	30.6	0.72	28.6	0.68	26.0
553 -570	25.9	0.74	29.9	0.71	27.8	0.69	26.8
570 -587	25.1	0.73	29.4	0.74	29.8	0.70	27.0
587 -604	24.6	0.67	25.5	0.71	28.0	0.69	26.8
604 -621	25.0	0.67	25.3	0.70	27.6	0.70	27.1
621 -638	26.3	0.67	25.6	0.71	28.2	n.d.	n.d.
638 -655	27.5	n.d.	n.d.	0.72	28.8	0.70	27.3
655 -672	27.8	0.70	27.6	0.71	28.1	0.69	27.0
672 -689	27.1	0.70	27.2	0.66	24.9	0.69	26.9
689 -705	26.4	0.70	27.6	0.68	26.2	0.67	25.1
***In situ* annual mean (°C)**	**26.4**						
Standard deviation		**0.02**	**1.5**	**0.02**	**1.1**	**0.01**	**0.8**
Flux weighted mean		**0.71**	**27.8**	**0.71**	**27.9**	**0.69**	**26.6**

Not determined (n.d.) were samples with too low amount of GDGTs for reliable TEX_{86} calculation

Table 3. TEX_{86} values, TEX_{86} temperature and flux weighted mean TEX_{86} temperature at the three trap deployment depth compared to *in situ* annual mean SST at the MS-3 station in the Arabian Sea. The average SST for each trap deployment time interval was calculated satellite date of the pathfinder Advanced Very High Resolution Radiometer (AVHRR) data set at http: podaac.jpl.nasa.gov.

1984]. In the northeastern Pacific upwelling site strong lateral advection was observed in meso-and bathypelagic realm [*Silver and Gowing* 1991] which may explain the observed substantial increase in the GDGT flux at 1500 m depth. This increase is probably derived from re-suspended sedimentary material transported in the Californian coastal current.

In the Arabian Sea lateral advection via eddies and filaments and re-suspension of sediments off the shallow Oman shelf can decouple deep water trap collections from surface processes [*Siegel and Deuser* 1997] and could be responsible for the flux maxima in the mid-water traps [*Honjo et al.* 1999, Wakeham et al., 2002]. Descending particles sampled in deep

water traps probably represent a complex mixture of particles derived from large areas. For instance, in the Arabian Sea the particle catchment areas might be as large as 10^3-10^4 km^2 (e.g. van *Gyldenfeld et al.,* 2000). Also the lateral transport of suspended sediments off the Arabian shelf may have an important influence in particle fluxes [*Witte and Pfannkuche*, 2002].

7.4.2 Seasonal variation in GDGT fluxes

At all three deployment depths the highest GDGT fluxes in the Arabian Sea time series were measured during the monsoon periods, especially during the SWM (Fig. 3a). This is consistent with previous studies were maximum fluxes of organic carbon and biomarker lipids occurred during the SWM, regardless of trap deployment depth and location [*Wakeham et al.,* 2002]. Phytol is a general biomarker for photoautotrophic plankton and in the Arabian Sea the highest GDGT fluxes occur at the same time as the highest phytol fluxes (Fig. 3b). This GDGT flux pattern seems in contradiction with the ecology of marine Crenarchaeota. Marine Crenarchaeota appear to be chemolithoautotroph (*Wuchter et al.,* 2003, *Herndl et al.,* 2005, *Wuchter et al.,* submitted) competing with phytoplankton for nutrients and their abundance is negatively correlated with that of phytoplankton as reported previously in different oceanic regimes [*Murray et al.,* 1998, 1999, *Massana et al.,* 1997, *Wuchter et al.,* submitted]. However, higher fluxes of GDGTs during SWM do not necessary imply a higher abundance of marine Crenarchaeota during the SWM. The relative increase in the GDGT flux between SI and SWM at 500 m is substantially smaller in comparison to that of specific biomarker lipids derived from photoautotroph organisms (i.e. diatoms and haptophytes) and even of total particles and organic carbon (Table 4). The high organic carbon flux during the SWM is caused by blooming photoautotrophs as a response to the increased levels of nutrients in the photic zone derived from upwelling waters. Major particulate mass fluxes occur at times of high primary productivity [*Wakeham and Canuel* 1988] because at that time a highly active food-web exists in the upper water column and a lot of phytoplankton derived particles settle down in deeper waters as marine snow. Thus, the higher amounts of GDGTs which are transported at that time to the sea floor are likely caused by the much more active food-web during the SWM, resulting in more efficient scavenging of archaeal cells, and not because of higher cell abundances of the marine Crenarchaeota.

Compounts	Origin	average SI flux $m^{-2}d^{-1}$	average SWM flux $m^{-2}d^{-1}$	rel. increase %
Total particle s		60 mg	361 mg	602
Organic carbon		6 mg	28 mg	443
Phytol	Phototrophs	5 µg	28 µg	552
C25:3 HBI	Rhisozolenoid diatoms	0.3 µg	17 µg	5360
C30 alkane 1,14 diol	Proboscia diatoms	3 µg	25 µg	952
37:2 alkenones	Haptophyts	0.4 µg	5 µg	1425
GDGTs	marine Crenarchaeota	4 µg	12 µg	276

Table 4. Average fluxes of different components during (SI) Spring Inter-monsoon and (SWM) South West monsoon at the 500 m trap at MS-3 station in the Arabian Sea.

7.4.3 TEX_{86} and size fraction

At the northeastern Pacific at both sampling sites no substantial variation in the TEX_{86} was observed in the different size classes of sinking particles (Table 2). The size fraction of the sinking particles <300µm consists of small passively sinking particles derived from the upper 100m , whereas the size fraction >300µm is probably mostly comprised of freshly produced fecal pellets of vertically migrating zooplankter which probably actively grazing on sinking large marine snow particles and descending algae [*Silver and Gowing* 1991]. The GDGT distribution and thus the TEX_{86} stay relatively invariant in the two size fractions. In the larger fraction the GDGTs are probably derived from Crenarchaeota which have been grazed and digested by zooplankton. Thus, our data show that alteration of GDGTs caused by grazing and digesting by heterotrophs does not change substantially the GDGT distribution.

7.4.4 Variations in TEX_{86} with depth

At the Arabian Sea traps and the northeast Pacific traps the TEX_{86} stayed relative invariant throughout the water column (Table 2 and 3). At both sampling sites the calculated TEX_{86} temperatures did not reflect in situ temperature at the different trap deployment depth but correlated best with the annual mean SST at these settings (Table 2 and 3). Interestingly, marine Crenarchaeota occur over a large depth range in the ocean [*Karner et al* 2001, *Herndl et al* 2005] and especially the GDGT signal of living crenarcheotal cells derived from the meso- and bathypelagic realm could influence the TEX_{86}. However, sinking particles like fecal pellets and marine snow aggregates having a high settling rate [*Wakeham and Canuel* 1988] and are mostly responsible for the vertical transport of material from the upper ocean to

the sea floor [*Wakeham and Canuel* 1988]. The similar TEX_{86} from the sinking particle fraction show that the GDGT signal is mostly derived from the upper part of the ocean and that the GDGT signal derived from deep water living Crenarchaeota do not contribute substantially to the GDGT sedimentary fluxes. This is consistent with previous studies on GDGTs in suspended POM from different oceanic regimes [*Wuchter et al.,* 2005], which shows that the TEX_{86} over a large depth range correlates best with SST rather than in situ temperature [*Wuchter et al* 2005]. In addition, a study of GDGTs in suspended POM and sediment traps from the Black Sea [*Wakeham et al.,* 2003] showed that high amounts of ^{13}C-depleted GDGTs in suspended POM in the deep anoxic zone could not be found in sediment traps and the underlying sediments. The authors suggested that due to the absence of grazing in the anoxic zone of the Black Sea, GDGTs biosynthesized in deep waters lack transport mechanisms to the sea floor, and thus the dominant GDGT flux occurs from the upper water column were an active food-web exists [*Wakeham et al.,* 2003].

7.4.5 Seasonal variation in TEX_{86}

The TEX_{86} measured at the shallow 500 m trap in the Arabian Sea showed a pronounced trend that follows that of the *in situ* SST, obtained by satellite observations (Fig. 4a), with an apparent offset of about three weeks. The time a particle need to sink and be captured in the 500 m trap likely causes this time offset in the TEX_{86} signal. Fine particles move through the water column at rates of 1-3 m day^{-1}[*Krishnaswami et al* 1981, *Bacon and Anderson*, 1982], whereas fecal pellets and marine snow may sink at rates of tens-to hundreds of m day^{-1} [e.g. *Small et al*., 1979, *McCave* 1984, *Asper,* 1987]. The signal that reaches the trap at 500 m is an integrated signal of particles of different size classes and sinking speed. The offset of ca. three weeks in the 500 m trap indicates that the captured particles move on average 25 m day^{-1} through the water column, and this is well in the range with the above mentioned particle sinking speeds. In the mid-water trap at 1500 m and the deep trap at 3000 m the TEX_{86} temperature signal does not show this pronounced seasonality as observed at the 500 m trap (Figs. 4b and c). The mid-water and deep trap are probably more influenced by lateral transport of particles and the GDGT signal that is captured in these traps rather reflects an integrated mixed GDGT signal derived from a larger area. In contrast, the trap at 500 m shows for the first time that the TEX_{86} is following the seasonal SST cycle demonstrating that

this proxy is excellently capturing upper water column temperatures. The TEX_{86} SST signal measured at 500 m depth is on average ca. 1°C higher than the SST measured *in situ*. This temperature offset could be caused due to the calibration equation used, which is derived from core tops. This calibration line possibly slightly overestimates SSTs at high temperatures such as those in the Arabian Sea. Indeed, when the equation derived from POM is used (Table 2) the SST estimates are ~1.5°C lower than *in situ* SST. Further development of these calibration line is required to see if there is a systematic off set between sediment traps and core tops or whether the calibration line needs to be further improved.

The calculated flux-weighted mean TEX_{86} SST in the three traps of the Arabian Sea deployed at different depth reflect annual mean SST (Table 3). The calculated flux-weighted mean TEX_{86} SSTs for the 500 and the 1500 m trap are ca. 1ºC higher than for the 3000 m trap (Table 3). The calculated annual mean *in situ* SST during the trap deployment period is nearly the same as the calculated flux-weighted mean TEX_{86} SST signal from the 3000 m trap (Table 3). This shows that even if in the upper parts of the water column the TEX_{86} in descending particles reflects seasonal SST the GDGT signal that reaches deep water and sediment reflects an integrated signal and the corresponding TEX_{86} reflects annual mean SST. This integrated signal is probably caused by the previously mentioned lateral transport and mixing mechanisms of organic matter in the Arabian Sea. Our results may thus explain why TEX_{86} in core top sediments from different geographic locations which correlates well with annual mean SST [*Schouten et al* 2002].

7.5 Conclusion

Our data show that the TEX_{86} signal in GDGTs contained in descending particles reflects SST and confirms that the GDGT signal which reaches the sediment is mainly produced in the upper water layer. The TEX_{86} is relatively invariant in different size fractions of descending particles throughout the water column, suggesting that alteration due to grazing and re-packaging of sedimentary GDGTs by zooplankton does not appear to substantially influence the GDGT distribution and thus the TEX_{86}. In the Arabian Sea time series we observed a strong correlation of the TEX_{86} in the upper 500 m trap with seasonal SST. The TEX_{86} signal which reaches the deep trap during the annual cycle was relatively invariant and reflected annual mean SST. This deep water temperature signal is probably strongly influenced from

lateral transport of particles and, therefore, the TEX_{86} in deeper waters or in sediment rather reflects an integrated annual mean SST rather than a seasonal SST signal. Our data presented here, in combination with previous studies on GDGT distributions in core top sediments [*Schouten et al.,* 2002], in suspended POM [*Wuchter et al*, 2005] and in mesocosms [*Wuchter et al.,* 2004], show the potential to use the TEX_{86} for reconstruction of upper water column temperatures in ancient environments.

7.6 Acknowledgements

We thank Martijn Woltering (NIOZ) for assistance in sample processing and Ellen Hopmans (NIOZ) for assistance and advice for the HPLC/MS analyses. Thanks also to numerous personnel who helped in sample collection during VERTEX and JGOFS cruises. The U.S. National Science Foundation supported the Arabian Sea cruise and the U.S. Office of Naval Research supported sample collection on VERTEX.

7.7 Literature list

Asper ,V.L. (1987), Measuring the flux and sinking speed of marine snow aggregates, *Deep-Sea Res. 34*, 1-17

Bacon, M. P. and R. F. Anderson (1982), Distribution of thorium isotopes between dissolved and particulate forms in the deep sea. *J. Geophys. Res. ,87,* 2045-2056.

DeLong, E. F. (1992), Archaea in coastal marine environments, *Proc. Natl. Acad. Sci.USA*, *89*, 5685-5689.

DeRosa, M. and A. Gambacorta (1988), The Lipids of Archaebacteria, *Prog. Lipid Res.*, *27*, 153-175.

Fuhrman, J. A., K. McCallum, and A. A. Davis (1992), Novel major archaebacterial group from marine plankton, *Nature*, *356*, 148-149.

Gliozzi, A., G. Paoli, M. De Rosa, and A. Gambacorta (1983), Effect of isoprenoid cyclization on the transition temperature of lipids in thermophilic archaebacteria. *Biochim. Biophys. Acta*, *735*, 234-242.

van Gyldenfeldt, A. B., J. Carstens, and J. Meincke (2000), Estimation of catchment area of sediment trap by measns of current meters and foraminiferal tests. *Deep-Sea Res. II, 47,* 1701-1717

Hoefs, M. J. L., S. Schouten, J. W. deLeeuw, L. L. King, S. G. Wakeham, and J. S. Sinninghe Damsté (1997), Ether lipids of planktonic archaea in the marine water column, *Appl. Environ. Microbiol.*, *63*, 3090-3095.

Honjo, S., J. Dymond, W. Prell, and V. Ittekkot (1999), Monsoon-controlled export fluxes to the interior of the Arabian Sea, *Deep-Sea Res. II 46*, 1859-1902

Herndl, G. J., T. Reinthaler, E. Teira, H. van Aken, C. Veth, A. Pernthaler and J. Pernthaler (2005), Contribution of Archaea to total prokaryotic production in the deep Atlantic Ocean. *Appl. and Environ. Microbiol, 71*, No.5.

Hopmans, E. C., S. Schouten, R. D. Pancost, M. T. J. Van der Meer, and J. S. Sinninghe Damsté (2000), Analysis of intact tetraether lipids in archaeal cell material and sediments by high performance liquid chromatography/atmospheric pressure chemical ionization mass spectrometry, *Rapid Commun. Mass Spectrom.*, *14*, 585-589.

Karl, D. M., P. A. LaRock, J. W. Morse and W. Sturges (1976), Adenosin triphosphate in the North Atlantic Ocean and its relationship to the oxygen minimum. *Deep-Sea Res., 23,* 81-88.

Karl , D. M. and G. A. Knauer (1984), Vertical distribution, transport and exchange of carbon in the northeast Pacific Ocean: evidence for multiple zones of biological activity. *Deep- Sea Res., 31,* 221-243.

Karner, M. B., E. F. DeLong, and D. M. Karl (2001), Archaeal dominance in the mesopelagic zone of the Pacific Ocean, *Nature*, *409*, 507-510.

Krishnaswami, S., M. M. Sarin and B. L. K. Somayajulu (1981), Chemical and radiochemical investigations of surface and deep particles of the Indian ocean, *Earth Planet. Sci. Lett., 54,* 81-96.

McCave, I. N. (1984), Size spectra and aggregation of suspended particles in the deep ocean, *Deep Sea Res.*, *31*, 329-352.

Massana R., A. E. Murray, C. M. Preston and E. F. DeLong (1997) Vertical distribution and phylogenetic characterization of marine planktonic Archaea in the Santa Barbara Channel. *Appl. Environ. Microbiol.*, *63,* 50-56.

Murray, A. E., C. M. Preston, R. Massana, L. T. Taylor, A. Blakis, K. Wu, and E. F. DeLong (1998), Seasonal and spatial variability of bacterial and archaeal assemblages in the coastal waters near Anvers Island, Antarctica, *Appl. Environ. Microbiol.*, *64,* 2585-2595.

Murray, A. E., A. Blankis, R. Massana, S. Strawzewski, U. Passow, A. Alldredge, and E. F. DeLong (1999), A time series assessment of planktonic archaeal variability in the Santa Barbara Channel. *Aquat. Microb. Ecol.*, *20*, 129-145.

Schouten, S., E. C. Hopmans, E. Schefuss, and J. S. Sinninghe Damsté (2002), Distributional variations in marine crenarchaeotal membrane lipids: a new tool for reconstructing ancient sea water temperatures?, *Earth. Planet. Sci Lett.*, *204*, 265-274.

Schouten, S., E. C. Hopmans, and J. S. Sinninghe Damsté (2004), The effect of maturity and depositional redox conditions on archaeal tetraether lipid palaeothermometry. *Org. Geochem., 35,* 567-571.

Siegel, D.A. and W.G. Deuser (1997), Deep ocean time-series particle trapping in the Sargasso Sea: the modelling of "statistical funnels". *Deep-Sea Res. I, 44,* 1519-1541.

Silver, M. W. and M.M. Gowing (1991), The "Particle" Flux: Origins and biological components, *Prog. Oceanog. 26,* 75-113.

Sinninghe Damsté, J. S., W. I. C. Rijpstra, E. C. Hopmans, F. Prahl, S. G. Wakeham, and S. Schouten (2002), Distribution of membrane lipids of planktonic *Crenarchaeota* in the Arabian Sea, *Appl. Environ. Microbiol.*, *68*, 2997-3002.

Small, L.F., S.W. Fowler and M.Y.Ünlü (1979), Sinking rates of natural copepod fecal pellets. *Mar. Biol.,51*, 233-241.

Smith, S., M. Roman, I. Prusova, K. Wishner, K. Gowing, L. A. Codispoti, R. Barber, J. Marra, and C. Flagg (1998), Seasonal response of zooplankton to monsoonal reveals in the Arabian Sea. *Deep-Sea Res. II, 45,* 2369-2403.

Uda, I., A. Sugai, Y. H. Itoh and T. Itoh (2001), Variation in molecular species of polar lipids from Thermoplasma acidophilum depends on growth temperature, *Lipids*, *36*, 103-105.

Urrère, M. A. and G. A. Knauer (1981), Zooplankton fecal pellet fluxes and vertical transport of particulate organic material in the pelagic environment. *J. Plankton Res., 3,* 369-387.

Wakeham, S. G. and E. A. Canuel (1988), Organic geochemistry of particulate matter in the eastern tropical North Pacific Ocean: Implications for particle dynamics, *J. Mar. Res.*, *46*, 183-213.

Wakeham, S. G. and C. Lee, Production, Transport, and Alteration of Particulate Organic Matter in the Marine Water Column, in *Organic Geochemistry*, edited by M. H. Engel and S. A. Macko, pp. 145-169, Plenum Press, New York, 1993.

Wakeham , S. G., M. L. Peterson, J. I. Hedges, and C. Lee (2002), Lipid biomarker fluxes in the Arabian Sea, with a comparison to the equatorial Pacific Ocean, *Deep-Sea Res. II, 49,* 2265-2301.

Wakeham, S. G., C. M. Lewis, E. C. Hopmans, S. Schouten, and J. S. Sinninghe Damsté (2003), Archaea mediate anaerobic oxidation of methane in deep euxinic waters of the Black Sea, *Geochim. Cosmochim. Acta*, *67*, 1359-1374.

Weller, R. A., M. M. Baumgartner, S. A. Josey, A. S. Fischer, and J. C. Kindler (1998), Atmospheric forcing in the Arabian Sea during 1994-1995: observations and comparisons with climatology and models. *Deep-Sea Res. II 45*, 1961-1999.

Wishner, K. F., M. M. Gowing, and C. Gelfman (1998), Mesozooplankton biomass in the upper 1000m in the Arabian Sea: overall seasonal and geographic patterns, and relationship to oxygen gradients. *Deep-Sea Res. II, 45,* 2405-2431.

Witte, U., and O. Pfannkuche (2002), High rates of benthic carbon remineralization in the abyssal Arabian Sea. *Deep-Sea Res. II*, *47*, 2785-2804.

Wuchter, C., S. Schouten, H. T. S. Boschker, and J. S. Sinninghe Damsté (2003), Bicarbonate uptake by marine Crenarchaeota, *FEMS Microbiol.Lett., 219*, 203-207.

Wuchter, C., S. Schouten, M.J.L. Coolen and J. S. Sinninghe Damsté (2004), Temperature dependent variation in the distribution of tetraether membrane lipids of marine Crenarchaeota: Implications for TEX_{86} paleothermometry. *Paleoceanography*, *19*, PA4028.

Wuchter, C., S. Schouten, S. G. Wakeham and J. S. Sinninghe Damsté (2005), Temporal and spatial variation in tetraether membrane lipids of marine Crenarchaeota in particulate organic matter: Implications for TEX_{86} paleothermometry. *Paleoceanography*, *20*, PA3013.

Wuchter, C., L. Herfort, M.J.L. Coolen, B. Abbas, P. Timmers, M. Strous, G.J. Herndl, J.J. Middelburg, S. Schouten and J. S. Sinninghe Damsté (2005), Ammonium oxidation by a member of marine Crenarchaeota, *Nature,* submitted.